Population and phase coherence during the growth of an elongated Bose-Einstein condensate

M. Hugbart, J. A. Retter, A. F. Varón, P. Bouyer,* and A. Aspect

*Laboratoire Charles Fabry de l'Institut d'Optique, CNRS, Université Paris-Sud, Campus Polytechnique,
RD128, 91127, Palaiseau cedex, France*

M. J. Davis

*ARC Centre of Excellence for Quantum-Atom Optics, School of Physical Sciences, University of Queensland,
Brisbane, Queensland 4072, Australia*

We study the growth of an elongated phase-fluctuating condensate from a nonequilibrium thermal cloud in the axially hydrodynamic regime, obtained by shock cooling. Quantitative measurements using momentum Bragg spectroscopy reveal the evolution of the phase coherence as the condensate grows to equilibrium. We find no delay between the population growth and the development of the phase coherence. We also compare the growth of the condensate with numerical simulations based on kinetic theory, revealing quantitative agreement except for an unexplained time delay.

PACS number(s): 03.75.Kk, 03.75.Nt

The nonequilibrium path to Bose-Einstein condensation is a complex process in which atoms accumulate in the ground state of the system and long-range phase coherence develops, resulting in a strong suppression of density fluctuations and a uniform phase. The kinetics of condensate formation has long been a subject of theoretical study, giving rise to a number of conflicting predictions (see [1] for a review). Quantitative theories have been formulated to model the condensate formation process in a harmonic trapping potential [2,3]. However, a limitation of these models is that the condensate is assumed to grow adiabatically in its phase coherent ground state. On the other hand, for a homogeneous system, Kagan *et al.* [4] proposed the appearance of a quasicondensate with strong phase fluctuations that die out on a time scale that increases with the size of the system. This homogeneous system description is also relevant to condensate growth in hydrodynamic clouds, where the trapping potential can be neglected [5]. Condensates in highly elongated traps, which can often be treated using the local density approximation, are expected to have properties close to the homogeneous case [6]. In addition, the axially hydrodynamic regime is easily attainable in such traps [7].

Experimentally, the problem of condensate formation has been approached by shock cooling [8–10] in harmonic traps: starting from a thermal cloud just above the transition temperature, rapid removal of the most energetic atoms from the trap results in an over-saturated thermal cloud. Subsequent thermalization leads to the growth of the condensate. Measurements of the growth of the condensed fraction in traps significantly less elongated than ours [8,9] have obtained good quantitative agreement with theory [12], but these experiments did not give access to the phase coherence of the growing condensate. The two-step growth curve reported in Ref. [9], and the growth of nonequilibrium, phase-fluctuating condensates from hydrodynamic clouds in Ref. [10] support the hypothesis of a quasicondensate during the initial stage

of condensate formation as proposed in Ref. [4]. However a recent experiment by Ritter *et al.* [11] studying the formation of long-range order in a Bose-Einstein condensate in a weak three-dimensional (3D) trap finds no evidence of a quasicondensate stage.

In this paper we present an experimental study of the evolution of both the condensate atom number and the phase coherence during the growth of a condensate in a highly elongated trap in the axially hydrodynamic regime. We observe that the population growth is in reasonable agreement with the predictions of kinetic theory, except for a delay that remain to be explained. We also use Bragg spectroscopy [13,14] to measure the coherence length during the growth of the condensate. Our observations are compatible with the scenario of Refs. [5,4], where a nonequilibrium quasicondensate is created at the onset of condensation and relaxes rapidly to equilibrium with shape oscillations. We find no evidence of supplementary phase fluctuations in the early stages of the growth, even at the shortest growth time for which we can perform the coherence measurements (100 ms).

In our experiment [15], we prepare a thermal cloud of ^{87}Rb atoms in the $5S_{1/2}|F=1,m_F=-1\rangle$ state in a Ioffe-Pritchard trap with final trap frequencies of $\omega_\perp = 2\pi \times 655(4)$ Hz radially and $\omega_z = 2\pi \times 6.53(1)$ Hz axially. Forced radio-frequency (rf) evaporation proceeds to a frequency $\Delta\nu_{rf} = 140$ kHz above that corresponding to the bottom of the combined magnetic and gravitational potential, giving an effective trap depth of $\varepsilon_i = 6\mu$K, and the rf knife is held at this value for a time varying from 1 to 12 s. This ensures thermal equilibrium, and allows us to control the atom number N_i in the range $(2.7-8.6) \times 10^5$. The resulting thermal cloud has a temperature T_i of about $\varepsilon_i/10$, just above the transition temperature T_c, which varies from 400 to 600 nK depending on the atom number.

We next shock-cool the cloud by rapidly ramping the rf knife to $\Delta\nu_{rf} = 40$ kHz in 25 ms, giving a final trap depth $\varepsilon_f = 1.5$ μK. The relative truncation rate $\dot{\varepsilon}/\varepsilon_f = 120$ s^{-1} is fast compared to the axial trap frequency, but slow compared to the radial trap frequency. In our elongated geometry this

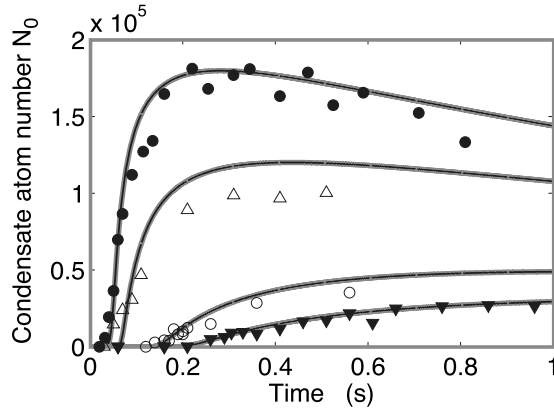*Electronic address: philippe.bouyer@institutoptique.fr

FIG. 1. Condensate growth curves for initial atom numbers: $N_i/10^5 = 8.6(9)$ ●, 7.2(7) △, 3.4(4) ○, and 2.8(5) ▼ [21]. Each point corresponds to an average over three experimental realizations. The lines are theoretical results of the model of [12], with a correction for the atom number calibration compatible with our systematic errors (20%). They have additional delay times of 10, 20, 50, and 50 ms respectively. The decrease in N_0 at longer times is due to three-body losses.

FIG. 2. Condensed fraction N_0/N and momentum width Δp as a function of t for an initial atom number $N_i = 3.8(3) \times 10^5$. [Open circles correspond to the data from Fig. 1 for $N_i = 3.4(3) \times 10^5$.] The decreasing momentum width indicates the growth of the coherence length with time. The dashed lines are guides to the eye. Some typical error bars are shown.

shock cooling results in a cloud transversally at equilibrium but axially out of equilibrium. The cloud tends toward local thermal equilibrium with a temperature $T < T_c$, in a time $\sim 3\tau_{coll} \lesssim 10$ ms [16] where τ_{coll} is the collision rate at the center of the trap [17]. Since the atom cloud is in the hydrodynamic regime axially ($\omega_z \tau_{coll} \ll 1$) [18], global equilibrium is reached on a time scale longer than the axial oscillation period.

In order to study the condensate growth, the cloud is held in the trap for a further time t after the end of the shock-cooling ramp, with the trap depth held constant at ε_f. We then switch off the trap and image the cloud after a 20 ms time of flight in order to obtain the total atom number N, temperature T, and condensate atom number N_0 [7,19]. By repeating the measurements at different times t for the same initial conditions, we obtain a growth curve for the condensate number, as shown in Fig. 1 for various initial atom numbers N_i [21]. At $t \simeq 20$ ms (depending on initial conditions), the atom number has dropped by 40% and the temperature is already below T_c, yet the condensate does not appear until later, with a delay time of 20–200 ms after the fast ramp.

We have simulated the evaporative cooling and condensate growth for our experiment based on the model described in [12] with the additional inclusion of three-body loss for the thermal cloud [20]. This method was in good quantitative agreement with experimental results for a less elongated system [9]. The results are shown in Fig. 1 and are in good quantitative agreement with the experimental data provided a delay time of 10–50 ms is added to better fit the experimental results. Apart from this there are no free parameters in our calculations, which are based on our measured data [21].

It is important to note that the simulation is not necessarily valid for such an elongated system in the hydrodynamic regime, nor does it take account of phase fluctuations. Indeed, our experiment is performed in an elongated trapping geometry, where temperature-dependent phase fluctuations c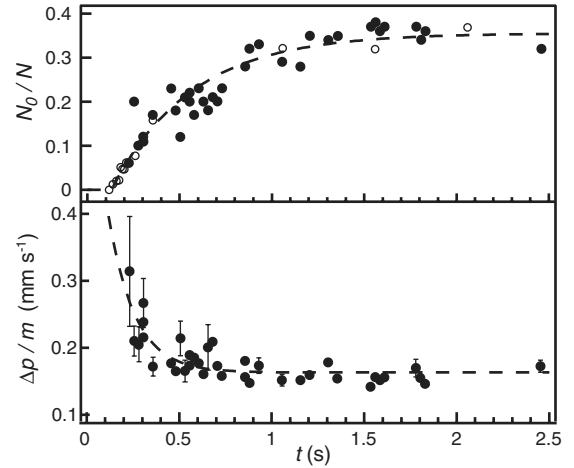an be present even at equilibrium [6,14,22–24]. For our parameters, the phase-coherence length $L_\phi = 15\hbar^2 N_0/16mk_B LT$ [6] at equilibrium is smaller than the condensate half-length L by a factor in the range 4–10, varying inversely with the condensate atom number. Given these considerations, it is perhaps surprising that the simulations bear any resemblance to the measurements. Two conclusions can nevertheless be drawn from the comparison. First, the growth of the condensed fraction is apparently delayed compared to the kinetic theory predictions, and this is unrelated to the efficiency of the cooling. Second, there is no evidence for a two-stage growth curve as was suggested in Ref. [9]. This shows that more work is still demanded to fully understand the growth of the Bose-Einstein condensate.

We now turn to our experimental study of the formation of phase coherence. We measure the coherence length of the condensate during its formation via its momentum distribution, using four-photon Bragg spectroscopy as described in Ref. [14]. At time t after the end of the shock-cooling ramp, the magnetic trap is switched off and after 2 ms of free expansion a 2 ms Bragg pulse is applied. The atoms are imaged after a further 16 ms time of flight, which allows separation of the diffracted atoms. The diffracted fraction is measured as a function of ν, the detuning between the Bragg beams which determines the velocity class diffracted, to obtain the momentum spectrum of the condensate. We fit a Lorentzian function to the measured spectra and extract the half width at half maximum (HWHM) $\Delta\nu = 2k_L \Delta p/2\pi m$, where m is the atomic mass, k_L the laser wave vector, and Δp the HWHM of the momentum distribution. For each spectrum, further images (typically 5) are taken without the Bragg pulses, from which the temperature T, condensate atom number N_0, and condensate half-length L are obtained.

The evolution of the momentum width Δp for an initial atom number $N_i = 3.8(3) \times 10^5$ is presented in Fig. 2 (lower panel). The corresponding condensed fractions are shown in the upper panel of Fig. 2 (filled circles). The momentum width Δp clearly decreases and thus the coherence length
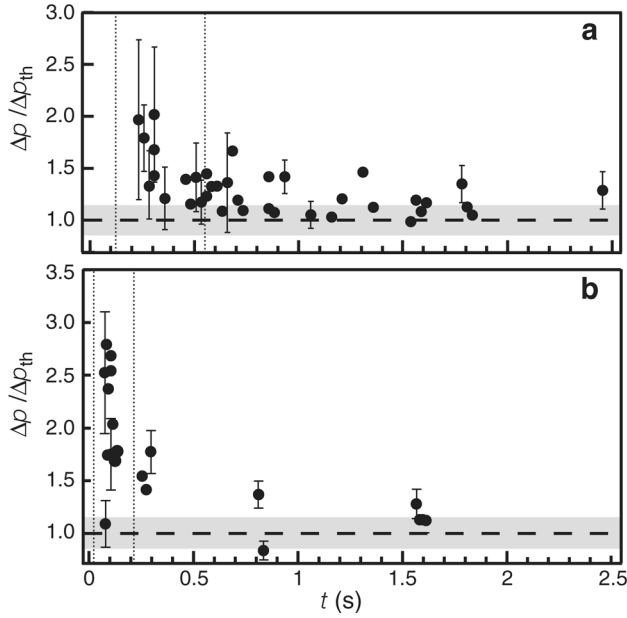
FIG. 3. Ratio of measured momentum width Δp to theoretical momentum width Δp_{th}, calculated for a condensate at equilibrium (see text) for $N_i =$ (a) $3.8(3) \times 10^5$ and (b) $7.2(3) \times 10^5$. (Data shown in (a) correspond to Fig. 2.) The condensate momentum width tends to the equilibrium value (dashed line) at long times. Some typical statistical error bars are shown; the gray band indicates systematic uncertainties on the equilibrium value. The first vertical line marks the onset of condensation; the second indicates the time at which the condensed fraction reaches $(1 - 1/e)$ of its final value.

increases. We know [14] that for a quasicondensate at thermal equilibrium, the coherence length increases with the number of atoms in the condensed fraction. More precisely, the momentum width follows [6,25]

$$\Delta p_{equ} = \hbar \sqrt{\left(\frac{2.04}{L}\right)^2 + \left(\frac{0.65}{L_\phi}\right)^2}, \qquad (1)$$

where the first term accounts for the Heisenberg-limited momentum width due to the finite size L of the condensate and the second term accounts for the presence of thermal phase fluctuations. The numerical factors account for integration over the 3D density profile. Equation (1) shows that, even if the condensate were at equilibrium at each instant during the growth, we would expect the momentum width to decrease with time, since both L_ϕ and L increase with the condensate atom number. We can therefore test whether the condensate coherence follows the density in this way. To do this accurately, we correct Δp_{equ} for the finite "instrumental width" of the Bragg spectrometer, by introducing as in [14] a Gaussian apparatus function of half-width $w_G = 200$ Hz. This results in a theoretical momentum width $\Delta p_{th} = \Delta p_{equ}/2 + \sqrt{(2\pi m/2k_L)^2 w_G^2 + (\Delta p_{equ}/2)^2}$. We then compare each measured momentum width Δp with the value Δp_{th} calculated for a condensate at equilibrium, using the parameters N_0, L, and T measured for each Bragg spectrum.

We plot the ratio $\Delta p / \Delta p_{th}$ in Fig. 3 for two different initial atom numbers. The dashed line at $\Delta p / \Delta p_{th} = 1$ indicates the value expected for a condensate always at equilibrium. Systematic uncertainties of 15% on this equilibrium value, mainly due to the atom number calibration (20%) and determination of w_G (10%), are represented by the gray band. Unambiguously, we observe that the ratio $\Delta p / \Delta p_{th}$ always lies above one (dashed line), and decreases in time. This indicates an excess momentum spread with respect to a condensate at equilibrium during the growth. As the condensate reaches equilibrium, the measurement dispersion decays and the momentum width tends to the predicted equilibrium value.

To interpret our results, we consider the scenario proposed by Kagan *et al.* [4] for condensate growth in a homogeneous system. The early stages of growth lead to a quasicondensate in which nonequilibrium, long-range phase fluctuations exist but density fluctuations are suppressed. The phase fluctuations then decay to produce the true phase-coherent condensate, with a characteristic time scale τ_ϕ which increases with the system size L: $\tau_\phi \propto L$ in the collisionless regime and $\tau_\phi \propto L^2$ in the hydrodynamic regime. Although our trapped system differs from the homogeneous system considered in Ref. [4], Svistunov [5] points out that this theory can be applied to trapped hydrodynamic clouds, where the trapping potential can be neglected. In this case, the resulting quasicondensate will be out of equilibrium with respect to a global coherent motion in the trap, thereby exciting a quadrupole mode similar to that observed in Refs. [10,14]. Indeed, for a higher atom number $N_i = 8.6 \times 10^5$ we directly observe quadrupole oscillations, with an amplitude (in the trap) of 12 μm and a decay constant of about 250 ms. The excess momentum widths in Fig. 3 can be attributed to such quadrupole oscillations with amplitudes of 4 μm ($N_i = 3.8 \times 10^5$) and 5.5 μm ($N_i = 7.2 \times 10^5$) [26] and decay constants of about 700 and 300 ms, respectively. These values are consistent with those obtained for $N_i = 8.6 \times 10^5$, assuming an oscillation amplitude and decay rate that increase with the atom number. Therefore, apart from this decaying quadrupole mode, we conclude that higher-order, nonequilibrium phase fluctuations have decayed within a time shorter than 100 ms after the onset of condensation, in qualitative agreement with the predictions of Kagan *et al.* [27].

In conclusion, our experimental observations of the population growth of an elongated condensate agree with numerical simulations, except for a yet unexplained time delay. Whether or not that delay is related to phase fluctuations in the thermal cloud is an open question. On the other hand, phase fluctuations in the condensed fraction do not seem to slow the rate of the population growth.

We have also directly observed the growth of the phase coherence with time by studying the evolution of the momentum width during condensate growth. Compared with that expected for a condensate at equilibrium, these measurements reveal a broadening of the momentum distribution during growth, compatible with quadrupole shape oscillations. Apart from this decaying oscillation, we conclude that the condensate has already reached the equivalent equilibrium coherence length within 100 ms after the onset of

condensation. Because a complete theory for our experimental situation is lacking, the comparison between theory and experiment can hardly be quantitative and an extension of the model of Ref. [4] to trapped condensates, particularly in this quasi-1D geometry [28], is required. In order to observe the decay of possible phase fluctuations at early times, a measurement of the phase coherence length at shorter times is needed. This is exceedingly difficult in our system, since at short times the condensed fraction is too small to obtain clear Bragg spectra. Other techniques might be used instead, such as atom laser correlation measurements [29], combined with single-atom detection [11,30,31].

[1] H. T. C. Stoof, J. Low Temp. Phys. **114**, 11 (1999).
[2] C. W. Gardiner, P. Zoller, R. J. Ballagh, and M. J. Davis, Phys. Rev. Lett. **79**, 1793 (1997); M. D. Lee and C. W. Gardiner, Phys. Rev. A **62**, 033606 (2000); M. J. Davis, C. W. Gardiner, and R. J. Ballagh, *ibid.* **62**, 063608 (2000).
[3] M. J. Bijlsma, E. Zaremba, and H. T. C. Stoof, Phys. Rev. A **62**, 063609 (2000).
[4] Yu. Kagan, B. V. Svistunov, and G. V. Shlyapnikov, JETP Lett. **75**, 387 (1992); Yu. Kagan and B. V. Svistunov, *ibid.* **78**, 187 (1994); Phys. Rev. Lett. **79**, 3331 (1997).
[5] B. Svistunov, Phys. Lett. A **287**, 169 (2001).
[6] D. S. Petrov, G. V. Shlyapnikov, and J. T. M. Walraven, Phys. Rev. Lett. **87**, 050404 (2001).
[7] F. Gerbier *et al.*, Phys. Rev. Lett. **92**, 030405 (2004).
[8] H.-J. Miesner *et al.*, Science **279**, 1005 (1998).
[9] M. Köhl *et al.*, Phys. Rev. Lett. **88**, 080402 (2002).
[10] I. Shvarchuck *et al.*, Phys. Rev. Lett. **89**, 270404 (2002).
[11] S. Ritter *et al.*, e-print cond-mat/0607102.
[12] M. J. Davis and C. W. Gardiner, J. Phys. B **35**, 733 (2002).
[13] J. Stenger *et al.*, Phys. Rev. Lett. **82**, 4569 (1999).
[14] S. Richard *et al.*, Phys. Rev. Lett. **91**, 010405 (2003).
[15] B. Desruelle *et al.*, Phys. Rev. A **60**, R1759 (1999).
[16] C. R. Monroe *et al.*, Phys. Rev. Lett. **70**, 414 (1993); H. Wu and C. J. Foot, J. Phys. B **29**, L321 (1996).
[17] Here, $1/\tau_{\text{coll}} = n_0 \sigma_{\text{el}} \bar{v}$, where n_0 is the peak atomic density, $\bar{v} = \sqrt{8 k_B T / \pi m}$ the thermal velocity, and $\sigma_{\text{el}} = 8 \pi a^2$ the cross section for elastic scattering, with m the atomic mass and a $=5.31(1)$ nm the *s*-wave scattering length [see E. G. M. van Kempen *et al.*, Phys. Rev. Lett. **88**, 093201 (2002)].
[18] For the thermal cloud immediately before the shock-cooling ramp, we obtain $0.04 < \omega_z \tau_{\text{coll}} < 0.13$.
[19] F. Gerbier *et al.*, Phys. Rev. A **70**, 013607 (2004).
[20] M. J. Davis (unpublished).
[21] All raw measured atom numbers N have been rescaled by a factor 0.8 in order to obtain better agreement between experiment and theory. This is consistent with our estimated uncertainty of 20% in our atom number measurements.
[22] S. Dettmer *et al.*, Phys. Rev. Lett. **87**, 160406 (2001).
[23] D. Hellweg *et al.*, Phys. Rev. Lett. **91**, 010406 (2003).
[24] M. Hugbart *et al.*, Eur. Phys. J. D **35**, 155 (2005).
[25] F. Gerbier *et al.*, Phys. Rev. A **67**, 051602(R) (2003).
[26] For such small amplitudes, the oscillations cannot be directly observed in the time-of-flight images due to the limited resolution of our imaging system.
[27] With our experimental parameters we calculate from [4] a damping time τ_ϕ between 10 and 500 ms, depending on the collisional regime.
[28] N. P. Proukakis, J. Schmiedmayer, and H. T. C. Stoof, Phys. Rev. A **73**, 053603 (2006).
[29] I. Bloch, T. W. Hänsch, and T. Esslinger, Nature (London) **403**, 166 (2000).
[30] A. Öttl, S. Ritter, M. Köhl, and T. Esslinger, Phys. Rev. Lett. **95**, 090404 (2005).
[31] M. Schellekens *et al.*, Science **310**, 648 (2005).